Bergeron Normand (Orcid ID: 0000-0003-2413-6810)

A potential growth thermal index (PGTI) for estimating juvenile Atlantic salmon (*Salmo salar*) size-at-age across geographical scales

Sébastien Ouellet-Proulx[1,2], Anik Daigle[1,3], André St-Hilaire[1], Carole-Anne Gillis[4], Tommi Linnansaari[5], Guillaume Dauphin[6], Normand Émile Bergeron[1]

[1]Eau Terre Environnement, Institut national de la recherche scientifique, Québec, QC, Canada

[2]Direction de la gestion intégrée de l'eau, Ministère de l'environnement et de la lutte contre les changements climatiques, Québec, QC, Canada

[3]CÉGEP Garneau, Québec, QC, Canada

[4]Gespe'gewaq Mi'gmaq Resource Council, Listuguj, QC, Canada

[5]Forestry and environmental management, University of New-Brunswick, Fredericton, NB, Canada

[6]Diadromous fish section, Department of fisheries and Oceans Canada, Moncton, NB, Canada

Correspondence

Normand Bergeron, Eau Terre Environnement, Institut national de la recherche scientifique, 490 rue de la Couronne, Québec (Québec) G1K 9A9 Canada

Email : normand.bergeron@inrs.ca

Funding information

This project was funded by a grant from the Atlantic Salmon Research Joint Venture and by the Fonds de recherche du Québec Nature et technologies, grant #208647.

1. Abstract

We present a potential growth thermal index (PGTI) and assess its correlation with juvenile Atlantic salmon *Salmo salar* fork length data collected near the end of the growth season in a range of latitudinal locations and geographic scales (watershed, regional, continental) across the American Northeast. The PGTI is based on two components: a water temperature-dependent growth curve, and a water temperature time series continuously describing the thermal environment preceding fish sampling. Testing various shapes and characteristics of the temperature-growth curve against fish length data revealed strong positive correlations for all combinations. PGTI Warming, calculated only from the beginning of the growth season until maximum summer temperature is reached, consistently performed well in explaining fish size-at-age across the latitudinal gradient and the three geographic scales that were considered. Varying thermal contrasts created by repeat sub-sampling of the dataset showed that fish length is better explained by the level of thermal contrast within the dataset than the geographical scale of analysis. A simple Generalized Linear Model (GLM) using a log link function with PGTI Warming, fish density and water discharge as predictors explained 87% of the variance of size-at-age of 0+ and 1+ juvenile Atlantic salmon.

Keywords: Atlantic salmon, GLM, growth, juvenile, Northeast America, thermal regime

2. Introduction

In the current context of climate change, water resources managers are facing the urgent need to redefine their decision-making tools. This is especially the case of fisheries managers in charge of cold-water species that are increasingly suffering from thermal habitat degradation. Studies showed that the anticipated warming of North American rivers could cause significant shifts in the spatial and temporal thermal habitat of cold water fish (Arismendi *et al.*, 2012; Isaak and Rieman, 2013). Quantifying potential growth is therefore a key element to the estimation of the recruitment of such species.

The effect of water temperature on growth of juvenile Atlantic salmon has received a fair share of attention in the last decades (e.g. Nicieza *et al.*, 1997; Nislow *et al.*, 2004; Bacon *et al.*, 2005; Strothotte *et al.*, 2005; Jonsson and Jonsson, 2009; Elliott and Elliott, 2010; Bal *et al.*, 2011; Imsland *et al.*, 2016; Sundt-Hansen *et al.*, 2018). Warmer temperature is generally acknowledged to have a positive effect on juvenile Atlantic salmon growth through several

factors: earlier emergence dates (Crisp, 1981; Skoglund *et al.*, 2011), earlier initial feeding time (Jensen *et al.*, 1991) and, most importantly, higher food consumption (Jonsson *et al.*, 2001; Elliott and Elliott, 2010).

Growth is mostly a continuous temperature-related process enabled by food consumption. Similarly, river water temperature is a continuous variable that depends on climatic, hydrologic and physiographic factors. However, most studies that have looked into the effect of water temperature on fish growth from field data summarized these continuous variables through various measures of central tendency (e.g. mean summer temperature, mean length of YOY). Summing degree-days of growth has been used in the past to alleviate this problem by integrating thermal variations occurring during the growth season (e.g. Steel *et al.*, 2012; Chezik *et al.*, 2014). The length of the growth season has been used to successfully model salmon age-at-smoltifcation. Symons (1979) predicted age-at-smoltifcation from the annual number of days with water temperature $> 7^{o}C$, while Power (1981) cumulated air temperature $> 5.6^{o}C$. Metcalfe and Thorpe (1990) showed that both temperature and day length are necessary to explain the geographical variations of age-at-smoltification because day length controls the daily amount of time available for feeding. Their model was able to collapse together age-at-smoltification data from streams spanning a range of latitudinal positions. Despite the overall good performance of the annual growth opportunity index they developed, the authors recognised that it failed to account for the fact that above a certain temperature threshold, salmonid growth slows down and eventually stops (Elliott 1982). Indeed, cumulating degree-days suggest that growth is linearly affected by water temperature, an assumption that was shown untrue by experimental work performed in previous studies (Jonsson *et al.*, 2001). Periods of critically high temperature can induce thermal stress to fish during which energy is primarily allocated to survival. These higher water temperature events can result in aggregation in cold refuges, reduced feeding efforts and reduced growth rates (e.g. Elliott, 1991; Dugdale *et al.*, 2016; Corey *et al.*, 2017).

Previous work also suggest that most of the juvenile growth occurs during the spring period (Jones et al., 2002; Martin-Smith and Armstrong, 2002; Bacon *et al.*, 2005; Gurner et al., 2008; Davidson *et al.*, 2010). Bacon et al. (2005) suggested that this result possibly reflects a trade-off between metabolic costs (greater at higher temperatures), food availability (which appears to peak in the spring) and appetite. In their longitudinal study of individual juvenile salmon growth in a small Scottish stream, they found that growth was positively correlated with temperature in

the spring because food availability was high and temperature relatively low. Accepting these findings leads to the assumption that growth rate is more likely to be affected by environmental variables early in the growth season.

Most studies pertaining to the growth of juvenile Atlantic salmon in relation to water temperature were carried out either in laboratory settings (e.g. Elliott and Hurley, 1997; Forseth *et al.*, 2001; Jonsson *et al.*, 2001; Skoglund *et al.*, 2011) or at a small spatial scale (e.g. Dion and Hughes, 2004; Arnekleiv *et al.*, 2006; Davidson *et al.*, 2010; Bal *et al.*, 2011). Recent work by Gregory *et al.* (2017) on two French and one English rivers suggest that water temperature has a stronger effect on growth of juvenile Atlantic salmon at a regional scale than at a watershed scale. Despite the large existing body of knowledge relating growth of juvenile Atlantic salmon to water temperature, only sparse information of these two components exist at more diverse and larger scales.

The objective of this paper is to investigate the control exerted by water temperature on the growth of juvenile of Atlantic salmon in North East America. We present a potential growth thermal index (PGTI) and assess its correlation with juvenile Atlantic salmon size-at-age. The analyses are performed at different scales ranging from the watershed to the continental scale. The specific objectives are to

1) Evaluate the statistical relationship between 0+ and 1+ juvenile Atlantic salmon size-at-age, and various water temperature metrics across North East America;
2) Investigate the sensibility of the selected temperature metrics across geographical scales;
3) Propose a simple model to predict juvenile salmon size-at-age for North American rivers based on temperature metrics and other abiotic and biotic variables.

3. Materials and Methods

Fish growth is best measured by sampling and measuring fish at the same location at different periods throughout the growth season (e.g. Jones et al., 2002; Davidson *et al.*, 2010). However, in this project, we used fork length near the end of the growth season as a proxy for growth. The general approach was to use continuous records of daily water temperature at each site to calculate various forms of temperature-dependent growth metrics up to the day that fish

sampling occurred, and to determine which metric performed best at explaining the variation of fish length across sites.

3.1. Water temperature and fish data collection

Fish length data of juvenile salmon at age 0+ and 1+ were collected through electrofishing surveys conducted by various agencies including the Department of Fisheries and Oceans of Canada (DFO), the Ministry of Forests, Fauna and Parks of Quebec (MFFP), the National Oceanic and Atmospheric Administration of the United States (NOAA). Sampling was also conducted for the present study as part of the Atlantic Salmon Research Joint Venture (ASRJV). Table 1 describes the data used for this study: watershed, source, number of sampling units (site-year) and number of 0+ and 1+ fish sampled. The locations of all sampling units are presented in Figure 1.

Although the fish sampling databases provided by our partners often comprised a large number of stations and years, only those fish samples corresponding to stations located less than 1 km away from an active thermograph (i. e. that had been collecting continuous water temperature records during the spring and summer periods preceding fish sampling) were kept for analysis. Although thermographs type and sampling interval varied slightly between data sets, they allowed the calculation of an accurate mean daily water temperature. In few instances, thermographs were installed after water temperature had already crossed the 5^{o}C mark. In those situations, a Gaussian function was fitted to the daily mean water temperature data available that year at that station and used to extrapolate temperature prior to thermograph installation. Prior to analysis, all water temperature series were analyzed to detect and filter out potential outliers due to thermograph malfunctioning or exposure to air. In order to reduce the risk of spatial covariance between sampling units, all stations were selected at least 1 km apart.

Most fish data were obtained from a single-pass open parcel electrofishing design (DFO, MFFP, ASRJV) although a mix of single-pass open parcels and multiple-pass closed parcels were used in one data set (NOAA). It is unlikely that these differences in sampling protocols caused any bias in the estimation of the distribution of fish size-at-age at each site. However, fish density estimates were necessarily larger at sites where a multiple-pass closed parcel design was used. In spite of this bias, it was decided that the value of keeping the fish length and water temperature data

from these sites outweighed the bias associated with the estimation of one of the explicative variables at a few sites.

3.2. PGTI definition and description of potential predictors

The potential growth thermal index (PGTI) we developed is based on two components: a continuous series of mean daily water temperature covering the entire growth season (Figure 2a) and a water temperature-dependent growth curve specific to each species and life-stages (Figure 2b). On this curve, potential growth coefficients range from 0 (thermal conditions that do not allow for growth) to 1 (optimal growth conditions). Daily potential growth values are obtained by reading from this curve the growth coefficient corresponding to the observed mean daily water temperature. The mean daily temperature is best calculated as the average of sub-hourly (e.g. 15 minutes) water temperature measurements. The information obtained can be used to describe the temporal variation of daily potential growth values (Figure 2c). Daily growth values can also be cumulated over the growth season to provide an index of the annual potential for growth, the PGTI (Figure 2d). PGTI values can be compared at different locations within a single river system (e.g. headwater vs main stem) or between river systems. Where future water temperature scenarios are available, the PGTI has the potential to be used to assess the impact of climate change on growth and age at smoltification.

The water temperature-dependant growth curve is often described using two functional forms: a trapezoidal-shaped curve obtained from laboratory experiments relating growth to temperature (Figure 2b solid line) (Elliott and Elliott, 2010), or a dome-shaped curve adapted from Mallet et al. (1999) (figure 2b dashed line), who added a temperature dependency to the growth coefficient of the von Bertalanffy growth model:

$$k = k_{opt} \frac{(T - T_{\min})(T - T_{\max})}{(T - T_{\min})(T - T_{\max}) - (T - T_{opt})^2} \quad (1)$$

where T is the daily water temperature, k is the growth rate (in days^{-1}), k_{opt} the growth rate at the temperature T_{opt} corresponding to optimal thermal conditions for growth, and T_{min} and T_{max} the temperature limits below and above which thermal conditions do not allow for growth. For instance, laboratory experiments on the growth of individual Atlantic salmon parr in the U.K.

and Norway (reviewed in Elliott and Elliott (2010)) revealed that they start feeding when temperature exceeds 6°C, that optimal growth conditions are found between 16 and 20°C and that individuals typically cease feeding when temperature exceeds 27°C (solid line in Figure 2b). The dome-shaped form of Mallet et al. (1999) used value of 6°C, 27°C and 18°C for T_{min}, T_{max}, and T_{opt}. In the current project, both the trapezoidal and dome shaped functions were tested with different values of T_{min}, T_{opt} and T_{max} (Table 2).

It is worth noting that these curves may be only applicable to circumstances where food availability is unlimited (Bacon et al., 2005). It was demonstrated that spring temperature has a positive effect on growth of juvenile Atlantic salmon (Bacon *et al.*, 2005; Arnekleiv *et al.*, 2006; Gregory *et al.*, 2017). Bacon et al. (2005) suggested that this positive relationship is driven by a combination of high food availability and appropriate water temperature during this season. In the northern hemisphere, the spring equinox represents the moment of the year with the longest daylight period, thereby providing more growth opportunities for juvenile salmon (Metcalfe and Thorpe, 1990) and possibly contributing to explain the positive association of springtime with growth. Therefore, a modified PGTI, called PGTI warming, was built. To create this new variable, mean daily water temperature series were smoothed using a seven-day moving average in order to remove small temperature variations. Then, the PGTI warming was calculated on the non-smoothed data from the beginning of the growth season until maximum summer temperature was reached.

The different PGTI formulations were compared in the analyses along with additional temperature-related metrics such as: cumulated degree-days between 6°C and 27°C (DD), mean springtime temperature (Tspring), mean summertime temperature (Tsummer), cumulated positive degree-days above during winter (WDD) (see Table 3). Beside temperature, previous studies have identified fish density and water discharge as important predictors of growth of juvenile Atlantic salmon (e.g. Power, 1981; Nislow *et al.*, 2004; Stradmeyer *et al.*, 2008; Davidson *et al.*, 2010). Although relative fish density (Dens) measurements were available at most sites, discharge (Q) was only available at a few locations. In order to obtain a complete and coherent dataset, an average annual volume of water was estimated from mean total precipitation (Rain) summed for the drainage area located upstream of each fishing site. Precipitation data were retrieved from WorldClim (Fick and Hijmans, 2017) on a 30 seconds grid (~ 1 km^2) derived from mean values measured between 1970-2000. Other potential predictors

analyzed included: the Julian day of individual fish sampling (DS) and river width at sampling location (Width) (Table 3). The probability distribution function of winter-degree-days, density, river width and discharge were highly skewed. Therefore, a log transformation was performed on all four variables.

3.3. Temperature and growth across scales

To evaluate the effect of temperature on growth at different geographic scales, the dataset was analysed at watershed, regional and continental scales across the distribution range of Atlantic salmon in North America. Only datasets with at least 10 sampling units were kept for the analysis. At the continental scale, all sites presented in Table 3 were kept for the analysis, representing a maximum span of 1500 km between the two sites farthest apart. At the regional scale, only sites below the 50th parallel were considered resulting in regions with a maximum span of 250 km. At the watershed scale, only the Miramichi and Restigouche watersheds had enough sites to be included in the analysis.

We have also investigated whether the ability of the PGTI to explain fish length was related to the magnitude of the thermal contrast between sites rather being solely related to their location. For this purpose, a subsample of sites (50% of the dataset) was randomly chosen 10 000 times from the continental scale dataset. The correlation coefficient and its p-value was then calculated and stored, along with the thermal contrast of the subsample. The thermal contrast was expressed as the difference between the maximum PGTI and minimum PGTI estimated.

3.4. PGTI parameters sensitivity

A sensitivity analysis was performed to determine which parameters of the thermal curve (T_{opt}, T_{min} and T_{max}) have the most influence on the correlation between PGTI and fish length. This was done by randomly sampling 1000 sets of parameters within the following ranges: T_{min} = [2; 10], T_{opt} = [12; 26] and T_{max} = [25; 28]. Each age class (0+ and 1+) was evaluated both separately and pooled together. The sensitivity analysis also allowed verifying if parameters based on purely statistical considerations yield the same parameters of the thermal curve than those obtained from laboratory work.

3.5. Modelling

Two different models were tested to predict fish size-at-age: a generalized linear model (GLM) and a generalized additive model (GAM). Those two models were selected for their straightforwardness, the flexibility of their implementation and their ease of interpretation. Both GLM and GAM have previously been used in fish ecology studies (e.g. Guisan *et al.*, 2002; Jokikokko *et al.*, 2006; Hrachowitz *et al.*, 2010; Drexler and Ainsworth, 2013).

In a GLM, the response variable is estimated using the sum of linear functions associated with each predictor and a link function. The standard formulation of a GLM is:

$$g\left(E\left(y\right)\right) = \beta_0 + \beta_1 x_1 + \beta_2 x_2 + \ldots + \beta_p x_p + \varepsilon \qquad 2$$

where β_i are coefficients, x_i are predictors, ε is the error term, g is the link function and $E(y)$ is the response variable. When the link function is the identity, the GLM is equivalent to a multiple linear regression.

The GAM model (Hastie and Tibshirani, 1986) is an extension of the GLM where the β_i are replaced by smoothing functions. As opposed to a GLM, a GAM does not rely on the assumption of a linear relationship between the predictors and the response variable. This allows for a better representation of nonlinear dependencies. The model can be expressed as:

$$g\left(E\left(y\right)\right) = \beta_0 + f_1\left(x_1\right) + f_2\left(x_2\right) + \ldots + f_p\left(x_p\right) + \varepsilon \qquad 3$$

where β_0 is the intercept and $f(x_i)$ is a smoothing function of the predictor x_i. One main advantage of the GAM over typical multiple linear model emanates from its capacity to represent different non-linear relationships between the predictors and the response variable (e.g. Laanaya *et al.*, 2017).

Both models were evaluated using a leave-one-out method based on Akaike information criterion (AIC), R^2, relative bias and mean absolute error (MAE). The choice of the best performing model was achieved using the AIC as it penalizes over parametrized models.

3.6. Ethical statement

For INRS researchers, the care and use of experimental animals complied with the Canadian Council on Animal Care (CCAC) animal welfare laws, guidelines and policies as approved by the

Comité Institutionnel de Protection des Animaux (CIPA) Protocol FOR-CPA 1708-03. UNB researchers worked under the DFO Gulf Region permit number SG-RHQ-17-142 and the UNB permit UNB AUP 17052. Historical electrofishing data from the Department of Fisheries and Oceans Canada (DFO) were collected following the directives, polices and Guidelines from the Canadian Council on Animal Care (CCAC). Historical electrofishing data from NOAA were obtained while operating under a Section 10 permit from the US Fish and Wildlife Service.

4. Results

4.1. Temperature and growth across scales

Figure 3 shows the correlation between temperature variables and length at three different geographic scales for 0+ and 1+ juvenile Atlantic salmon. At the continental scale (i.e. all sites included), the most correlated variable when 0+ and 1+ fish are pooled together is PGTI warming with r = 0.94. For 1+ fish, mean spring temperature (April through June) yields the highest correlation coefficient with r = 0.81 while PGTI (6, 16, 20, 27) was the most correlated with fish length for 0+ with r = 0.69. At the regional scale, 0+ length was also significantly correlated to water temperature metrics, with the highest correlation yielded by PGTI (6, 16, 20, 27) with r = 0.66. For 1+ fish, correlation was maximized with PGTI Dome-shaped (8, 20, 29), with r = 0.53. At the watershed scale, PGTI dome-shaped (6, 18, 27) and PGTI (6, 16, 20, 27) returned the highest correlation for 0+ fish on the Restigouche (r = 0.81) while PGTI (8, 18, 22, 29) returned the best correlation on the Miramichi (r = 0.69). Analysis of 1+ fish was not conducted at the watershed scale due to an insufficient number of sampling units.

These results indicate that, according to the available data, fish length is positively correlated with water temperature at all geographic scales for 0+ and 1+ Atlantic salmon. For most datasets, PGTI Warming is better correlated to fish length than the other temperature metrics tested. According to the results shown in Figure 3, the magnitude of the correlation is not related to the scale of the study area, with higher correlation coefficients between PGTI and fish length observed at the watershed scale (r = 0.81 on the Restigouche) compared to the continental scale (r = 0.69). The relationship between PGTI Warming and fish length at all sites is presented in Figure 4. These relationships can be represented by linear functions, also displayed on the graph.

The scale of analysis was assessed in terms of distance but also of thermal contrast. Figure 5 shows that the magnitude of thermal contrast within a dataset has a strong influence on the correlation between PGTI Warming and juvenile Atlantic salmon size-at-age. The relationship between the correlation coefficient of PGTI warming and fish length (y-axis), and the standard deviation (STD) of the dataset followed an asymptotic curve with a R^2 of 0.53. Both the randomly sampled data and the subsample data followed the asymptote with some deviations for lower STD of PGTI Warming values. The inflection point of the asymptote was observed at a STD of 15.26 PGTI warming days. When a dataset had a thermal contrast below this value, a mean correlation of 0.65 (STD = 0.22) was observed (Figure 5) while a mean correlation of 0.94 (STD = 0.04) was observed for STD PGTI Warming above the inflection point. This indicates a stabilisation of the relationship between thermal regime and fish length when the thermal contrast is above the inflection point.

4.2. PGTI parameters sensitivity

Figure 6 shows PGTI Warming parameters sensitivity for 0+ and 1+ fish and 0+ and 1+ fish pooled together. It can be seen that T_{opt} parameters are more sensitive than T_{min} and T_{max} for all age classes. For 0+ fish, correlation increases with T_{opt} until it reaches 16°C (correlation coefficient = 0.66; T_{min} = 8.1°C; T_{max} = 27.9°C). Correlation showed a 1% variation when T_{opt} varied between 16-18°C. For 1+ fish, maximum correlation coefficient (0.81) was obtained at T_{opt} = 21.8°C (T_{min} = 2°C; T_{max} = 28°C). Most variation in correlation (0.35-0.70) was observed when T_{opt} was lower than 18.5°C. When 0+ and 1+ are pooled together, maximum correlation coefficient (0.94) was obtained for T_{opt} = 19.1°C (T_{min} = 2.2°C; T_{max} = 27.9°C). Little to no variation in maximum correlation coefficient is induced by T_{min} and T_{max}. The general pattern seen on Figure 6 was also found when the other datasets were used independently.

4.3. Modelling

Models were built using a combination of a temperature statistic, a physiographic variable and fish density. For the temperature statistic, PGTI Warming was selected because of its higher correlation with fish length compared to the other temperature metrics tested (Figure 3). For the physiographic variable, log discharge and log river width yielded similar correlation coefficients (Figure 3) and were highly correlated with each other (corr. coef. = 0.9). Discharge was selected for subsequent modelling. Thus, various combination of PGTI Warming, log

discharge and density were tested using GLM and GAM models. Table 4 presents performance criteria (AIC, R^2, relative bias and Mean Absolute Error (MAE)) for the three model formulations tested.

According to AIC, the best performing model for both fish classes pooled together (0+ and 1+; AIC = 616.52; R^2 = 0.87) as well as 1+ alone (AIC = 433.06; R^2 = 0.88) was the GLM with respectively an identity link and a log link function, with PGTI Warming, Density and Discharge as predictors. For 0+ fish, GLM with a log link function, with PGTI DS and Discharge provided as inputs (AIC = 156.8; R^2 = 0.52), performed better than the other models. Overall, the GLM models outperformed the GAM models for all age classes. No bias was observed in all models (< 0.01 – 0.02; Table 4). Poorer performances were observed when 0+ fish were modelled alone compared to 1+, and 0+ and 1+ together. Model coefficients of the GLM –log model are presented in Table 5. The models were primarily driven by the temperature variable (β = 0.2399) followed by similar contribution of density (β = -0.0295) and discharge (β = -0.0305).

The scatter plot on Figure 7a shows the goodness of fit between modelled and measured fish length. Data points follow the bisector line indicating no major bias throughout the dataset. Scatter increases with fish length suggesting greater estimation error for larger fish. However, scatter plot of absolute relative residuals (Figure 7b) shows that residuals magnitude is proportional to fish length. A Grubbs test (Grubbs, 1950) was applied (α = 0.05) to trace the presence of outliers in absolute relative residuals and highlight sites where the models yield higher errors. Three sites were highlighted for both GLM and GAM. Two were from the Restigouche watershed (DFO dataset) and one from the Miramichi watershed (ASRJV dataset). Two of those sites (Restigouche watershed) hosted the smallest fish of the whole dataset (< 40 mm) and were sampled earlier than 95% of the other sites.

5. Discussion

5.1. Temperature and growth across scales

The results of this study show a clear relationship between the thermal regime of North American river and juvenile Atlantic salmon size-at-age. Different formulations of the PGTI are effective at summarizing growth potential according to thermal river conditions. Growth rate of juvenile Atlantic salmon is known to influence the age at which juveniles will migrate to sea (e.g. Metcalfe and Thorpe, 1990; Strothotte *et al.*, 2005). Reliable relationship linking temperature

and size-at-age can thus greatly help predicting potential salmon production in a changing climate.

The good performance of PGTI Warming to explain size-at-age is coherent with results obtained by Jonsson *et al.* (2001). This can be explained by the fact that higher growth rates are observed at the beginning of the growth season (e.g. Martin-Smith and Armstrong, 2002; Bacon *et al.*, 2005) which corresponds to a warming period in rivers. Seasonal patterns of feeding behavior of juvenile Atlantic salmon (e.g. Metcalfe et al., 1986) can also explain higher growth rates in early summer induced by higher feeding motivation during this period.

Contrasting results were found for European salmon populations where the highest growth rate of juvenile salmon was observed between July and September (Sanchez-Hernandez et al., 2016). However, before July, water temperature below critical temperature for growth were observed in the rivers where fish were sampled. This suggests that water temperature during spring and early summer was the major controlling factor impeding food consumption and growth. Forseth et al. (2001) demonstrated the influence of water temperature on energy intake and growth for Norwegian salmon populations. They showed that a critical temperature acts as a trigger for both food consumption and growth with a slight desynchronization between the two mechanisms. Such results point towards a combined influence of seasonal factors and thermal thresholds to trigger food consumption and growth.

Another potential explanation for PGTI Warming being the best predictor of size-at-age is the positive relationship between temperature during eggs incubation and emergence date, initial feeding and subsequent growth (Crisp, 1981; Crisp, 1988; Jensen *et al.*, 1991; Skoglund *et al.*, 2011), including winter river temperature (Finstad and Jonsson, 2012).

Although PGTI Warming is somewhat better correlated to size-at-age than the other thermal variables of the present study, most forms of PGTI were well suited to predict juvenile salmon size at various scales. Hence, future work using a variant of the PGTI should consider the entirety of the growth season.

In opposition to results obtained in previous research by Gregory *et al.* (2017), water temperature did not show greater correlation to fish length at larger geographic scales. However, the significant influence of the thermal contrast of a dataset on the correlation between PGTI warming and fish length (Figure 5) suggests that the level of spatial thermal

heterogeneity dictates at which level water temperature affects growth over other predictors. In homogeneous thermal conditions, other drivers such as physiographic, hydrologic or population structure predictors will more likely have a higher relative influence. However, the present study demonstrated the potential of PGTI to evaluate thermal quality of juvenile Atlantic salmon habitats at smaller scales.

5.2. PGTI parameters sensitivity

Previous studies that assessed salmonid growth potential based on water temperature either established optimal growth temperatures from laboratory experiments (e.g. Elliott and Hurley, 1997; Forseth *et al.*, 2001; Jonsson *et al.*, 2001) or used fixed parameters in a model along with covariates to estimate growth (Fontoura and Agostinho, 1996; Dion and Hughes, 2004; Bal *et al.*, 2011). This study showed the sensitivity of T_{opt} to the statistical relationship between PGTI Warming and juvenile Atlantic salmon size-at-age. The optimal values obtained for 0+ fish, around 16°C, were within the same range of temperature reported in the literature (i.e. 16-20°C in Elliott and Elliott, 2010). For 1+ fish, T_{opt} was considerably higher (21.8°C) than for 0+, exceeding optimal temperatures reviewed in Elliott and Elliott (2010). However, T_{opt} was more sensitive for values below 18°C. In both age classes, correlation was more sensitive to reducing T_{opt} values rather than increasing it.

One important limitation of the present study is the inability to indicate if the fish sampled really experienced the temperatures recorded by the thermal logger or if they have exploited different thermal habitats during their growth period. The presence or absence of thermal refuges in the proximal environment of the sites and their use by juveniles as noted in previous work (e.g. Dugdale *et al.*, 2016) also limits the possible inferences on mechanisms linking thermal stress and growth. Additional work relating internal fish temperature and growth would be of interest to fully capture the consequences of high temperatures on growth of juvenile Atlantic salmon.

5.3. Modelling

A simple GLM using a log link function with PGTI Warming, density and discharge as predictors was able to explain 87% of the variance of size-at-age of 0+ and 1+ juvenile Atlantic salmon. Previous modelling efforts were conducted on a single river reach or a single watershed (Forseth *et al.*, 2001; Dion and Hughes, 2004; Arnekleiv *et al.*, 2006; Davidson *et al.*, 2010; Bal *et al.*, 2011). In this study, we were able to predict juvenile Atlantic salmon size-at-age across a large

portion of North American Atlantic salmon population distribution for two age classes (0+ and 1+). Such model can be useful to predict the recruitment potential of North American salmon rivers in future climates. For instance, growth trajectories can be used to estimate size-at-age according to hydrological and population characteristics from which age at emigration can be inferred (Figure 8). The possible modifications of these trajectories at given sites can be investigated using climatic model projections. Data availability limited the extent of this study to 0+ and 1+ fish. However, long-term watershed monitoring of all age classes from emergence to smoltification would allow the establishment of population specific growth trajectories and thus refine our knowledge of juvenile Atlantic salmon response to climate change.

6. Conclusion

In the present study, we proposed a simple and straightforward temperature index to describe size-at-age of 0+ and 1+ juvenile Atlantic salmon through various implementations of the PGTI. The warming phase of the river thermal regime allowed to explain most of the growth variance of juvenile salmon through the PGTI Warming. This temperature index consistently performed well in explaining fish size-at-age across the three geographic scales (watershed, regional, continental) analyzed. Correlation between thermal regime and fish length was shown to be mostly dependant on the level of thermal contrast of the dataset rather than on the geographical scale of analysis. The results demonstrate the relevance of using water temperature characteristics to predict growth potential at any given geographic scale in contrasted thermal environments. Growth trajectories were established based on thermal regimes, juvenile salmon density and discharge using a simple GLM. Such model can be implemented in conjunction with climate change scenarios to help predict the response juvenile Atlantic salmon changing thermal environments.

7. Acknowledgement

We wish to thank the following persons for their assistance in the field: Antoine Boudry, Jérémie Boudreault, Marc-André Pouliot, André Boivin. Sincere thanks to these organizations for their contribution to the realization of the project: Centre Interuniversitaire de Recherche sur le saumon atlantique (CIRSA), Canadian Rivers Institute (CRI), DFO, Restigouche River Watershed Management Committee). The help and support of Patricia Edwards and Doug Bliss from the Atlantic Salmon Research Joint Venture was much appreciated throughout the project.

8. Contributions

Ideas: SO-P, AD, ASH, NEB

Data generation: SO-P, C-AG, MC, TL, GD

Data analysis: SO-P

Manuscript preparation: SO-P, NEB

Funding: NEB

9. Significance statement

The role of water temperature on fish growth is becoming increasingly important due to global warming, but no simple thermal metric exists to relate fish growth to species-specific temperature-dependent growth curve. The potential growth thermal index (PGTI) developed in this study successfully estimated juvenile Atlantic salmon size-at-age from a range of latitudinal locations and geographic scales (watershed, regional, continental) across the American Northeast. The PGTI could be used in combination with climate change scenarios to estimate the future trajectory of ectotherm aquatic species.

10. References

Arismendi, I., Johnson, S. L., Dunham, J. B., Haggerty, R., & Hockman-Wert, D. (2012). The paradox of cooling streams in a warming world: regional climate trends do not parallel variable local trends in stream temperature in the Pacific continental United States. *Geophysical Research Letters*, *39*(10). DOI: 10.1029/2012GL051448

Arnekleiv, J. V., Finstad, A. G., & Rønning, L. (2006). Temporal and spatial variation in growth of juvenile Atlantic salmon. *Journal of Fish Biology*, *68*(4), 1062-1076

Bacon, P. J., Gurney, W. S. C., Jones, W., McLaren, I. S., & Youngson, A. F. (2005). Seasonal growth patterns of wild juvenile fish: partitioning variation among explanatory variables, based on individual growth trajectories of Atlantic salmon (Salmo salar) parr. *Journal of Animal Ecology*, *74*(1), 1-11

Bal, G., Rivot, E., Prévost, E., Piou, C., & Baglinière, J. L. (2011). Effect of water temperature and density of juvenile salmonids on growth of young-of-the-year Atlantic salmon Salmo salar. *Journal of Fish Biology*, *78*(4), 1002-1022

Chezik, K. A., Lester, N. P., & Venturelli, P. A. (2014). Fish growth and degree-days I: selecting a base temperature for a within-population study. *Canadian Journal of Fisheries and Aquatic Sciences*, *71*(1), 47-55

Corey, E., Linnansaari, T., Cunjak, R. A., & Currie, S. (2017). Physiological effects of environmentally relevant, multi-day thermal stress on wild juvenile Atlantic salmon (Salmo salar). *Conservation physiology*, *5*(1). DOI: 10.1093/conphys/cox014

Crisp, D. T. (1981). A desk study of the relationship between temperature and hatching time for the eggs of five species of salmonid fishes. *Freshwater biology*, *11*(4), 361-368.

Crisp, D. T. (1988). Prediction, from temperature, of eyeing, hatching and 'swim-up'times for salmonid embryos. *Freshwater biology*, *19*(1), 41-48.

Davidson, R. S., Letcher, B. H., & Nislow, K. H. (2010). Drivers of growth variation in juvenile Atlantic salmon (Salmo salar): an elasticity analysis approach. *Journal of Animal Ecology*, *79*(5), 1113-1121.

Dion, C. A., & Hughes, N. F. (2004). Testing the ability of a temperature-based model to predict the growth of age-0 Arctic grayling. *Transactions of the American Fisheries Society*, *133*(4), 1047-1050.

Drexler, M., & Ainsworth, C. H. (2013). Generalized additive models used to predict species abundance in the Gulf of Mexico: an ecosystem modeling tool. *PloS one*, *8*(5).

Dugdale, S. J., Franssen, J., Corey, E., Bergeron, N. E., Lapointe, M., & Cunjak, R. A. (2016). Main stem movement of A tlantic salmon parr in response to high river temperature. *Ecology of freshwater fish*, *25*(3), 429-445.

Elliott, J. M. (1982). The effects of temperature and ration size on the growth and energetics of salmonids in captivity. *Comparative Biochemistry and Physiology Part B: Comparative Biochemistry*, *73*(1), 81-91.

Elliott, J. M. (1991). Tolerance and resistance to thermal stress in juvenile Atlantic salmon, Salmo salar. *Freshwater Biology*, *25*(1), 61-70.

Elliott, J., & Elliott, J. A. (2010). Temperature requirements of Atlantic salmon Salmo salar,

brown trout Salmo trutta and Arctic charr Salvelinus alpinus: predicting the effects of climate change. *Journal of fish biology*, *77*(8), 1793-1817.

Elliott, J. M., & Hurley, M. A. (1997). A functional model for maximum growth of Atlantic salmon parr, Salmo salar, from two populations in northwest England. *Functional Ecology*, *11*(5), 592-603.

Fick, S. E., & Hijmans, R. J. (2017). WorldClim 2: new 1-km spatial resolution climate surfaces for global land areas. *International journal of climatology*, *37*(12), 4302-4315.

Finstad, A.G., & Jonsson, B. (2012). Effect of incubation temperature on growth performance in Atlantic salmon. *Marine Ecology Progress Series*, *454*, 75-82.

Fontoura, N. F., & Agostinho, A. A. (1996). Growth with seasonally varying temperatures: an expansion of the von Bertalanffy growth model. *Journal of Fish Biology*, *48*(4), 569-584.

Forseth, T., Hurley, M. A., Jensen, A. J., & Elliott, J. M. (2001). Functional models for growth and food consumption of Atlantic salmon parr, Salmo salar, from a Norwegian river. *Freshwater biology*, *46*(2), 173-186.

Gregory, S. D., Nevoux, M., Riley, W. D., Beaumont, W. R., Jeannot, N., Lauridsen, R. B., ... & Roussel, J. M. (2017). Patterns on a parr: Drivers of long-term salmon parr length in UK and French rivers depend on geographical scale. *Freshwater Biology*, *62*(7), 1117-1129.

Grubbs, F. E. (1950). Sample criteria for testing outlying observations. *The Annals of Mathematical Statistics*, *21*(1), 27-58.

Guisan, A., Edwards Jr, T. C., & Hastie, T. (2002). Generalized linear and generalized additive models in studies of species distributions: setting the scene. *Ecological modelling*, *157*(2-3), 89-100.

Gurney, W. S., Bacon, P. J., Tyldesley, G., & Youngson, A. F. (2008). Process-based modelling of decadal trends in growth, survival, and smolting of wild salmon (Salmo salar) parr in a Scottish upland stream. *Canadian Journal of Fisheries and Aquatic Sciences*, *65*(12), 2606-2622.

Hastie, T. J. (2017). Generalized additive models. In *Statistical models in S* (pp. 249-307).

Routledge.

Hrachowitz, M., Soulsby, C., Imholt, C., Malcolm, I. A., & Tetzlaff, D. (2010). Thermal regimes in a large upland salmon river: a simple model to identify the influence of landscape controls and climate change on maximum temperatures. *Hydrological Processes*, *24*(23), 3374-3391.

Imsland, A.K., Pettersen, K., Stefansson, S. (2016). Growth and smoltification of three Norwegian strains of Atlantic salmon *Salmo salar* reared under different thermal regimes. *River research and applications,* **22**: 1085–1095

Isaak, D. J., & Rieman, B. E. (2013). Stream isotherm shifts from climate change and implications for distributions of ectothermic organisms. *Global Change Biology*, *19*(3), 742-751.

Jensen, A. J., Johnsen, B. O., & Heggberget, T. G. (1991). Initial feeding time of Atlantic salmon, Salmo salar, alevins compared to river flow and water temperature in Norwegian streams. *Environmental biology of fishes*, *30*(4), 379-385.

Jokikokko, E., Kallio-Nyberg, I., Saloniemi, I., & Jutila, E. (2006). The survival of semi-wild, wild and hatchery-reared Atlantic salmon smolts of the Simojoki River in the Baltic Sea. *Journal of Fish Biology*, *68*(2), 430-442.

Jones, W., Gurney, W. S., Speirs, D. C., Bacon, P. J., & Youngson, A. F. (2002). Seasonal patterns of growth, expenditure and assimilation in juvenile Atlantic salmon. *Journal of Animal Ecology*, 916-924.

Jonsson, B., & Jonsson, N. (2009). A review of the likely effects of climate change on anadromous Atlantic salmon Salmo salar and brown trout Salmo trutta, with particular reference to water temperature and flow. *Journal of fish biology*, *75*(10), 2381-2447.

Jonsson, B., Forseth, T., Jensen, A. J., & Næsje, T. F. (2001). Thermal performance of juvenile Atlantic Salmon, Salmo salar L. *Functional Ecology*, *15*(6), 701-711.

La Laanaya, F., St-Hilaire, A., & Gloaguen, E. (2017). Water temperature modelling: comparison between the generalized additive model, logistic, residuals regression and linear regression models. *Hydrological sciences journal*, *62*(7), 1078-1093.

Mallet, J. P., Charles, S., Persat, H., & Auger, P. (1999). Growth modelling in accordance with daily water temperature in European grayling (Thymallus thymallus L.). *Canadian Journal of Fisheries and Aquatic Sciences*, *56*(6), 994-1000.

Martin-Smith, K. M., & Armstrong, J. D. (2002). Growth rates of wild stream-dwelling Atlantic salmon correlate with activity and sex but not dominance. *Journal of Animal Ecology*, *71*(3), 413-423.

Metcalfe, N. B., Huntingford, F. A., & Thorpe, J. E. (1986). Seasonal changes in feeding motivation of juvenile Atlantic salmon (Salmo salar). *Canadian Journal of Zoology*, *64*(11), 2439-2446.

Metcalfe, N. B., & Thorpe, J. E. (1990). Determinants of geographical variation in the age of seaward-migrating salmon, Salmo salar. *The Journal of Animal Ecology*, 135-145.

Nicieza, A. G., & Metcalfe, N. B. (1997). Growth compensation in juvenile Atlantic salmon: responses to depressed temperature and food availability. *Ecology*, *78*(8), 2385-2400.

Nislow, K. H., Sepulveda, A. J., & Folt, C. L. (2004). Mechanistic linkage of hydrologic regime to summer growth of age-0 Atlantic salmon. *Transactions of the American Fisheries Society*, *133*(1), 79-88.

Power, G. (1981). Stock characteristics and catches of Atlantic salmon (Salmo salar) in Quebec, and Newfoundland and Labrador in relation to environmental variables. *Canadian Journal of Fisheries and Aquatic Sciences*, *38*(12), 1601-1611.

Sánchez-Hernández, J., Gabler, H. M., Elliott, J. M., & Amundsen, P. A. (2016). Use of a growth model to assess the suboptimal growth of Atlantic salmon parr in a subarctic river. *Ecology of freshwater fish*, *25*(4), 518-526.

Skoglund, H., Einum, S., Forseth, T., & Barlaup, B. T. (2011). Phenotypic plasticity in physiological status at emergence from nests as a response to temperature in Atlantic salmon (Salmo salar). *Canadian Journal of Fisheries and Aquatic Sciences*, *68*(8), 1470-1479.

Steel, E. A., Tillotson, A., Larsen, D. A., Fullerton, A. H., Denton, K. P., & Beckman, B. R. (2012). Beyond the mean: The role of variability in predicting ecological effects of stream temperature on salmon. *Ecosphere*, *3*(11), 1-11.

Stradmeyer, L., Höjesjö, J., Griffiths, S. W., Gilvear, D. J., & Armstrong, J. D. (2008). Competition between brown trout and Atlantic salmon parr over pool refuges during rapid dewatering. *Journal of Fish Biology*, *72*(4), 848-860.

Strothotte, E., Chaput, G. J., & Rosenthal, H. (2005). Seasonal growth of wild Atlantic salmon juveniles and implications on age at smoltification. *Journal of Fish Biology*, *67*(6), 1585-1602.

Sundt-Hansen, L. E., Hedger, R. D., Ugedal, O., Diserud, O. H., Finstad, A. G., Sauterleute, J. F., ... & Forseth, T. (2018). Modelling climate change effects on Atlantic salmon: Implications for mitigation in regulated rivers. *Science of the Total Environment*, *631*, 1005-1017.

Symons, P. E. (1979). Estimated escapement of Atlantic salmon (Salmo salar) for maximum smolt production in rivers of different productivity. *Journal of the Fisheries Board of Canada*, *36*(2), 132-140.

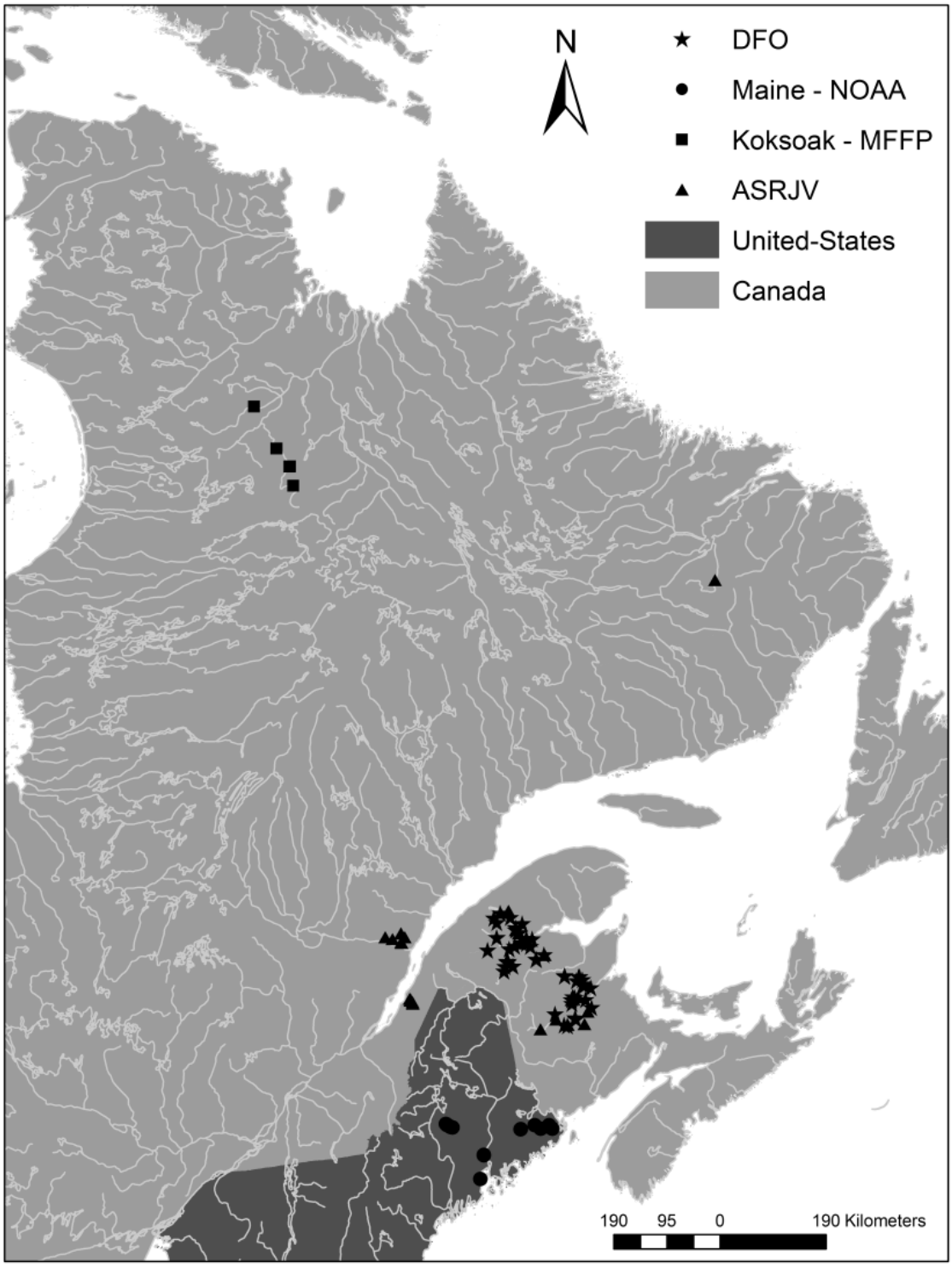

Figure 1. Map of sampling sites according to data source.

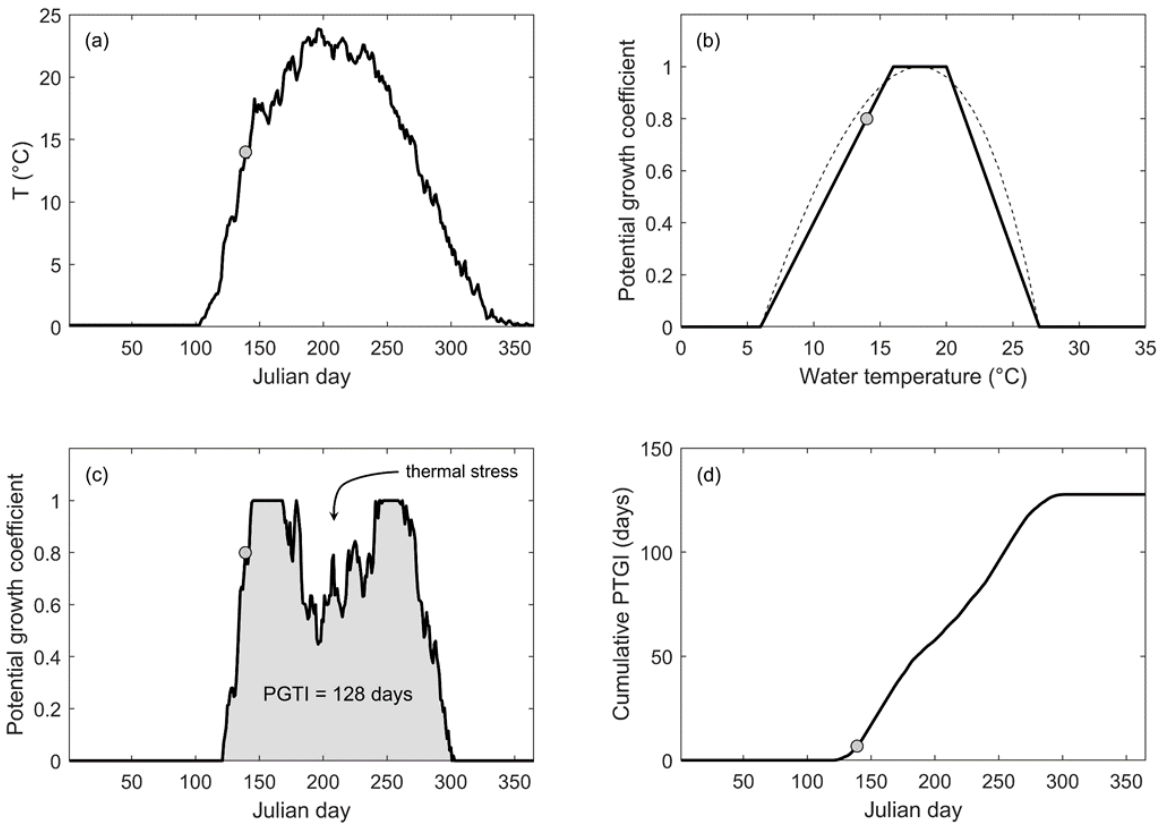

Figure 2. Calculation of the PGTI requires A) a continuous series of mean daily water temperature covering the entire growth season, and B) a water temperature-dependent growth curve specific to the species and life-stage analysed. Two curves for juvenile Atlantic salmon were used in the study: a trapezoidal curve (solid line) obtained by interpolating between the temperature limits reported by Elliott & Elliott (2010) and the dome-shaped curve (dashed line) adopted by Mallet et al. (1999). C) Daily potential growth values are obtained by reading from the temperature-dependent growth curve the growth coefficient corresponding to the observed mean daily water temperature. Repeating this calculation for every day of the data set provides a description of the temporal variation of daily potential growth values throughout the growth season. D) Daily growth values can be cumulated over the growth season to provide an index of the annual potential for growth.

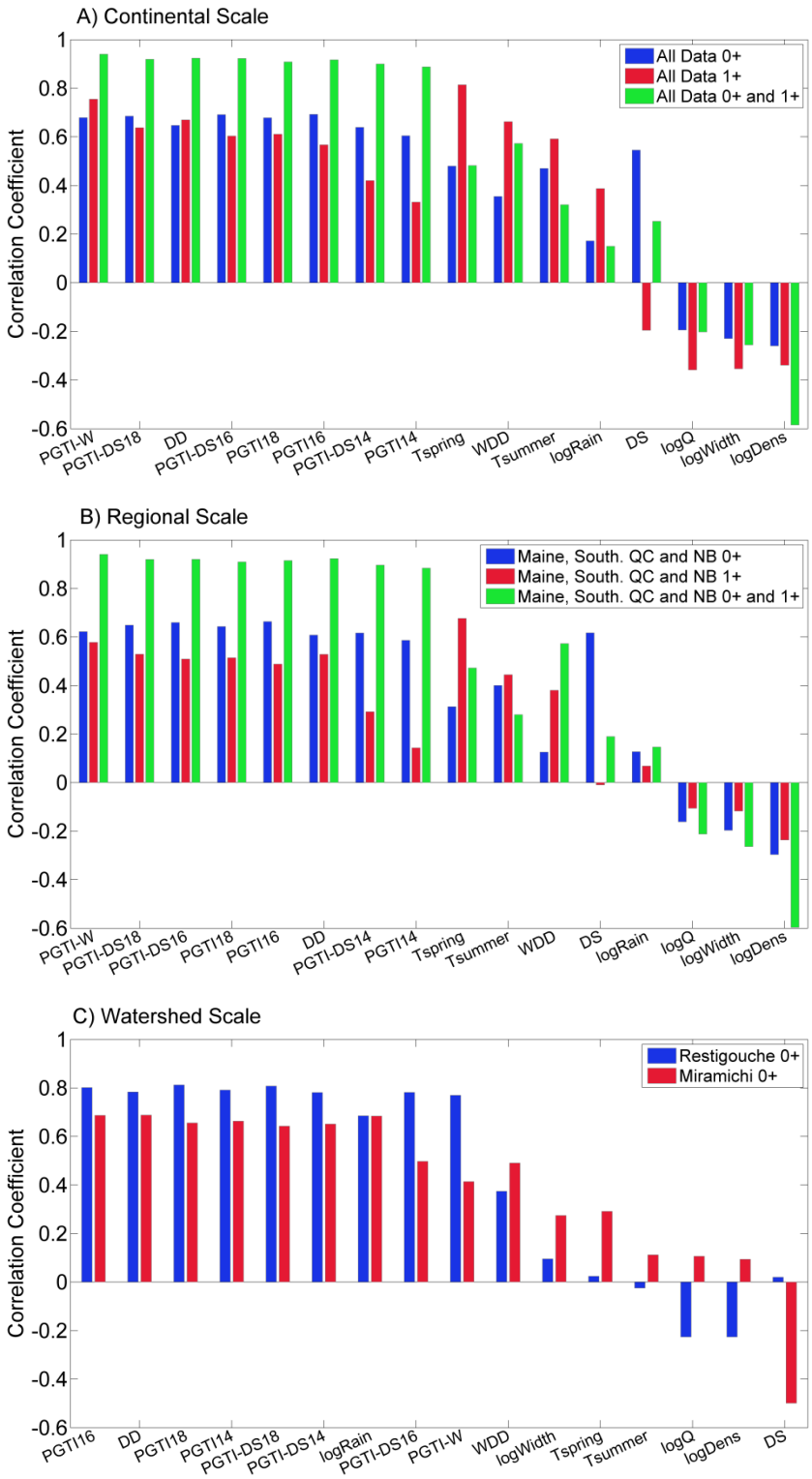

Figure 3. Sorted correlation coefficients of temperature variables listed in Table 3 and fork length of 0+ and 1+ juvenile Atlantic salmon at A) the continental, B) the regional and C) the watershed scale.

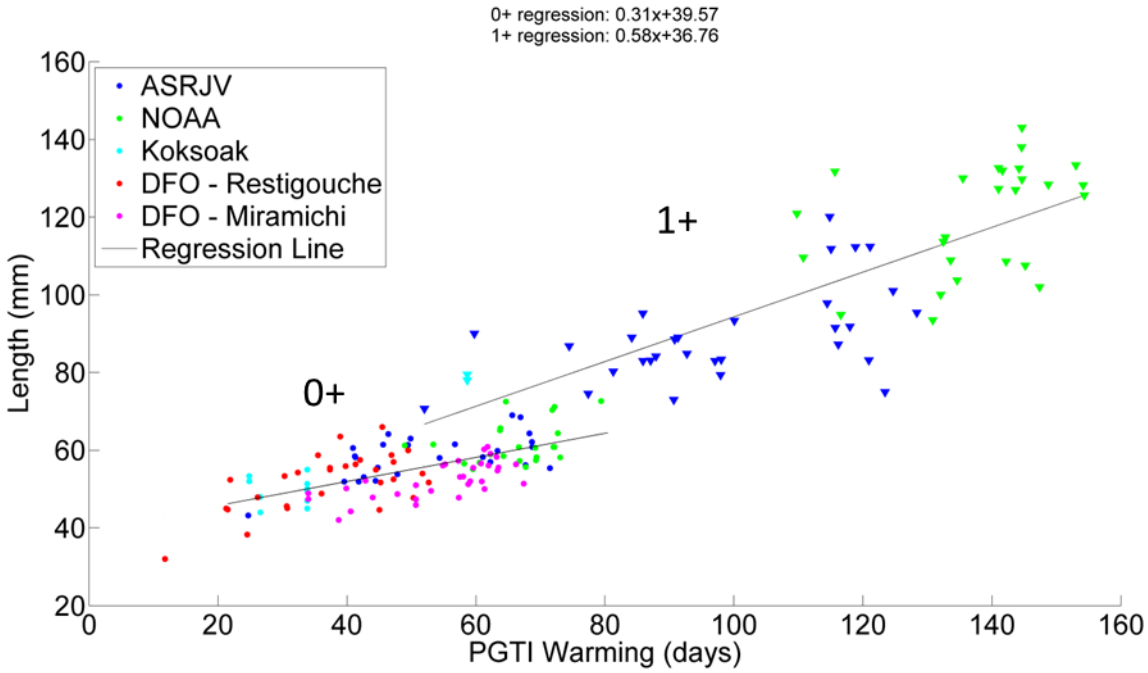

Figure 4. Juvenile Atlantic salmon fork length as a function of PGTI warming for 0+ (circles) and 1+ fish

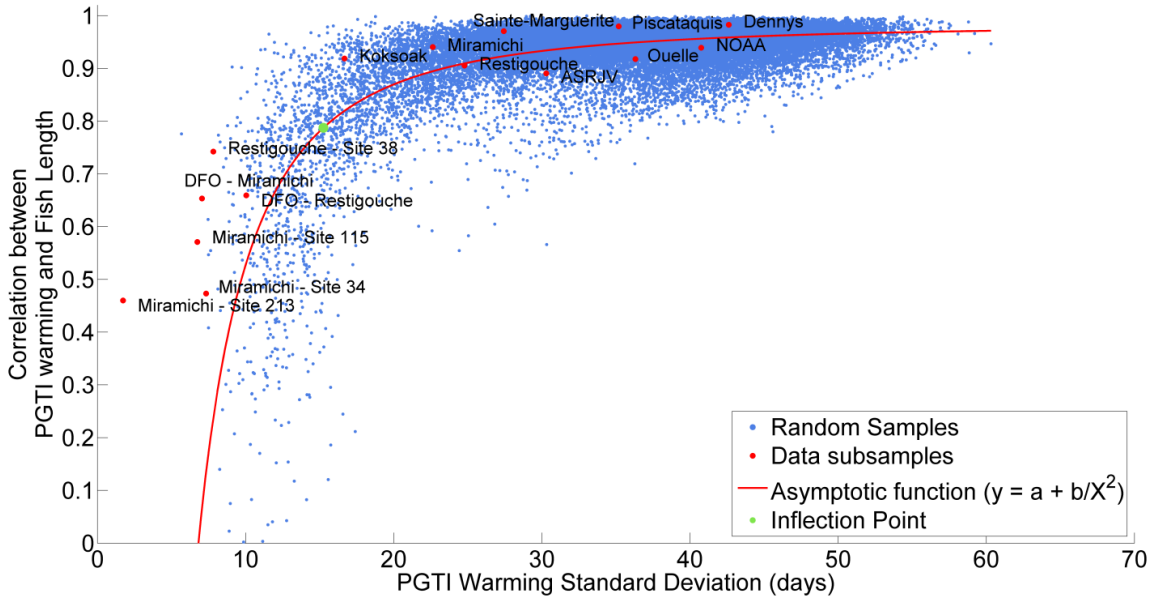

Figure 5. A) Scatter plot of the standard deviation of PGTI Warming and the correlation between PGTI Warming and fish length for random samples of 20 sampling units 0+ and 1+ (blue) and subsamples of datasets, watersheds and sites (red).

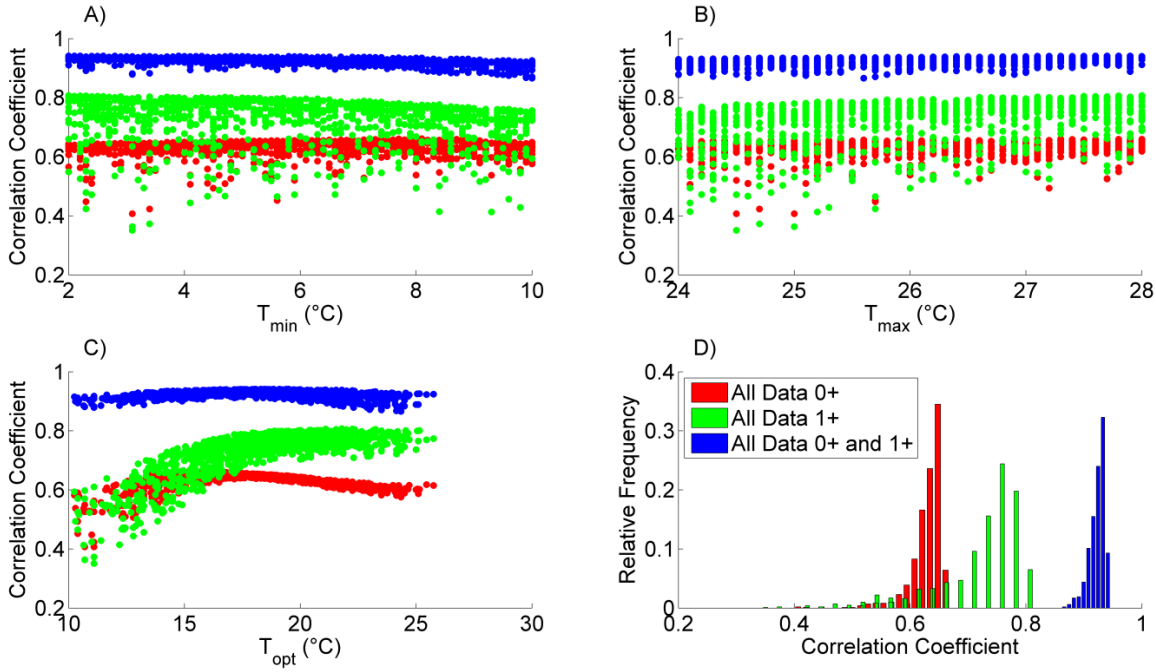

Figure 6. Scatter plots of correlation coefficients and PGTI Warming parameters A) Tmin, B) Tmax and C) Topt for 0+ (red), 1+ (green) and 0+ and 1+ (blue) fish and D) their correlation coefficients distribution.

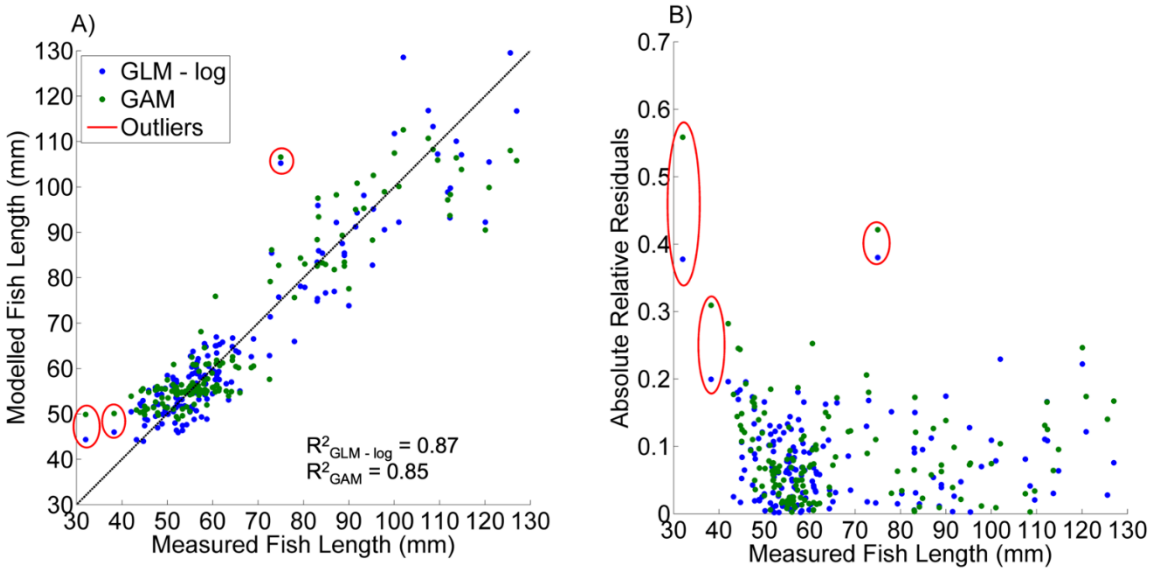

Figure 7. A) Scatter plot of modelled fish length compared to measured fish length and B) absolute relative residuals according to fish length. Outliers were calculated on absolute relative residuals.

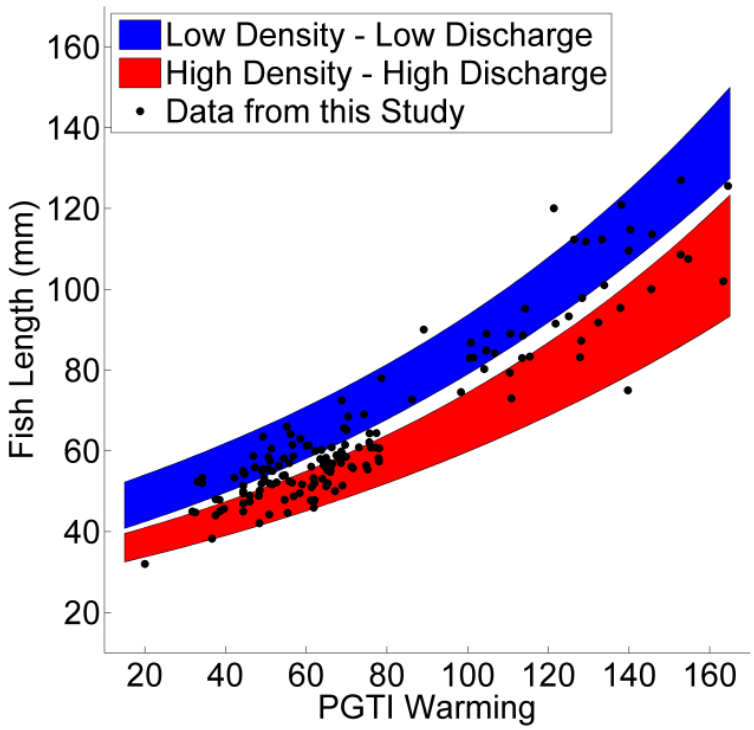

Figure 8. Confidence intervals (95%) of growth trajectories as function of PGTI Warming of low density and low discharge sites (blue) and high density and high discharge sites (red).

Figure 1. Map of sampling sites according to data source.

Figure 2: Calculation of the PGTI requires A) a continuous series of mean daily water temperature covering the entire growth season, and B) a water temperature-dependent growth curve specific to the species and life-stage analysed. Two curves for juvenile Atlantic salmon were used in the study: a trapezoidal curve (solid line) obtained by interpolating between the temperature limits reported by Elliott & Elliott (2010) and the dome-shaped curve (dashed line) adopted by Mallet et al. (1999). C) Daily potential growth values are obtained by reading from the temperature-dependent growth curve the growth coefficient corresponding to the observed mean daily water temperature. Repeating this calculation for every day of the data set provides a description of the temporal variation of daily potential growth values throughout the growth season. D) Daily growth values can be cumulated over the growth season to provide an index of the annual potential for growth.

Figure 3. Sorted correlation coefficients of temperature variables listed in Table 3 and fork length of 0+ and 1+ juvenile Atlantic salmon at A) the continental, B) the regional and C) the watershed scale.

Figure 4. Juvenile Atlantic salmon fork length as a function of PGTI warming for 0+ (circles) and 1+ fish (triangles).

Figure 5. A) Scatter plot of the standard deviation of PGTI Warming and the correlation between PGTI Warming and fish length for random samples of 20 sampling units 0+ and 1+ (blue) and subsamples of datasets, watersheds and sites (red).

Figure 6. Scatter plots of correlation coefficients and PGTI Warming parameters A) Tmin, B) Tmax and C) Topt for 0+ (red), 1+ (green) and 0+ and 1+ (blue) fish and D) their correlation coefficients distribution.

Figure 7. A) Scatter plot of modelled fish length compared to measured fish length and B) absolute relative residuals according to fish length. Outliers were calculated on absolute relative residuals.

Figure 8. Confidence intervals (95%) of growth trajectories as function of PGTI Warming of low density and low discharge sites (blue) and high density and high discharge sites (red).

Table 1 : List of watersheds included in the study with the source of the data, the number of sampling units (site-year) and the number of fish per age class.

Data Source	Watershed	Number of Sampling Units	Number of 0+ fish	Number of 1+ fish
DFO	Restigouche	29	315	0
	Miramichi	41	534	0
ASRJV	Ouelle	5	43	85
	Restigouche	6	85	47
	Miramichi	8	137	93
	Ste-Marguerite	7	125	84
	Kenamu	1	9	17
MFFP	Koksoak	10	30	16
NOAA	Dennys	4	101	21
	Ducktrap	1	30	6
	East Machias	2	25	39
	Machias	2	9	26
	Penobscot	2	60	35
	Piscataquis	10	364	103
Total		**128**	**1867**	**572**

Table 2: Different temperature-growth curves tested. The interpolation models are linear interpolations between the indicated temperature limits (see Figure 1); the functional form of the dome-shaped curve is defined in Bal et al. (2011).

Model	T_{min} (°C)	T_{max} (°C)	T_{opt} (°C)
Trapezoidal	6	27	16-20
Trapezoidal	4	25	14-18
Trapezoidal	8	29	18-22
Dome-shaped	6	27	18
Dome-shaped	4	25	16
Dome-shaped	8	29	20

Table 3. List of potential predictors of juvenile Atlantic salmon length

Variable	Abbreviation	Description	Units
PGTI (4, 14, 18, 25)	PGTI14	Interpolated potential Growth Thermal Index for Tmin = 4°, Tmax = 25°C and Topt = 14-18°C	Days
PGTI (6, 16, 20, 27)	PGTI16	Interpolated potential Growth Thermal Index for Tmin = 6°, Tmax = 27°C and Topt = 16-20°C	Days
PGTI (8, 18, 22, 29)	PGTI18	Interpolated potential Growth Thermal Index for Tmin = 8°, Tmax = 29°C and Topt = 18-22°C	Days
PGTI Dome-shaped (4, 16, 25)	PGTI_DS14	Dome-shaped potential Growth Thermal Index for Tmin = 4°, Tmax = 25°C and Topt = 26°C	Days
PGTI Dome-shaped (6, 18, 27)	PGTI_DS16	Dome-shaped potential Growth Thermal Index for Tmin = 6°, Tmax = 27°C and Topt = 18°C	Days
PGTI Dome-shaped (8, 20, 29)	PGTI_DS18	Dome-shaped potential Growth Thermal Index for Tmin = 8°, Tmax = 29°C and Topt = 20°C	Days
PGTI Warming (6, 18, 27)	PGTI_W	Interpolated potential Growth Thermal Index for Tmin = 6°, Tmax = 27°C and Topt = 18°C when water temperature is increasing	Days
Day of Sampling	DS	Julian day of sampling	Julien day
Degree Days	DD	Cumulated degree day between 6°C and 27°C	°C
Mean Temp. April-June	Tspring	Mean temperature during the month of April through June	°C
Mean Temp. July-August	Tsummer	Mean temperature during the month of July and August	°C
Winter Degree Days	WDD	Cumulated degree day above 0°C during the month of November through May	°C
log Density	Dens	Log transformed juvenile Atlantic salmon density	log number of fish/100 m^2
log Width	Width	Log transformed river width	log mm
log(Yearly Rain)	Rain	Log transformed mean yearly total precipitation	log mm
log Yearly Discharge	Q	Log transformed mean yearly total discharge	log m^3/year

Table 4. Performance criteria of juvenile Atlantic salmon size-at-age for two GLM and a GAM. Framed boxes represent best model/predictors combinations according to AIC

Predictors	Age class	AIC			R^2			Relative Bias			Mean Absolute Error MAE; mm)		
		GLM - Identity	GLM - log	GAM	GLM - Identity	GLM - log	GAM	GLM - Identity	GLM - log	GAM	GLM - Identity	GLM - log	GAM
PGTI Warming	0+	179.38	162.85	184.27	0.23	0.44	0.25	< 0.01	< 0.01	0.02	4.59	3.75	4.10
	1+	437.35	442.36	450.38	0.87	0.87	0.87	0.01	0.01	< 0.01	6.46	6.44	6.29
	0+ 1+	626.01	624.93	645.59	0.86	0.86	0.84	< 0.01	< 0.01	< 0.01	5.83	5.53	5.83
PGTI Warming Density	0+	182.94	166.89	185.21	0.20	0.41	0.26	0.01	< 0.01	< 0.01	4.65	4.07	4.22
	1+	437.02	442.40	451.74	0.88	0.87	0.87	< 0.01	< 0.01	< 0.01	6.32	6.25	6.17
	0+ 1+	625.98	625.17	646.12	0.86	0.86	0.84	< 0.01	< 0.01	< 0.01	5.76	5.52	5.83
PGTI Warming Discharge	0+	178.26	158.99	187.64	0.27	0.50	0.32	< 0.01	0.01	< 0.01	4.41	3.82	3.97
	1+	434.85	440.57	454.64	0.88	0.88	0.87	< 0.01	< 0.01	0.01	6.47	6.12	6.12
	0+ 1+	620.78	619.74	651.12	0.87	0.87	0.85	< 0.01	< 0.01	< 0.01	5.77	5.44	5.69
PGTI Warming	0+	182.04	164.19	188.29	0.24	0.46	0.30	0.02	0.01	< 0.01	4.48	3.82	4.02
Density	1+	433.06	437.69	455.07	0.88	0.88	0.87	< 0.01	< 0.01	< 0.01	6.30	6.12	6.11
Discharge	0+ 1+	619.05	616.52	650.03	0.87	0.87	0.85	< 0.01	< 0.01	< 0.01	5.69	5.34	5.69
PGTI DS (6, 18, 27)	0+	167.55	163.50	181.05	0.38	0.43	0.27	0.01	0.02	0.01	4.00	3.77	4.12
	1+	461.17	461.43	458.15	0.84	0.84	0.86	< 0.01	0.01	0.01	7.12	7.01	6.73
	0+ 1+	651.55	650.46	653.55	0.84	0.84	0.83	< 0.01	< 0.01	0.01	6.07	5.92	6.07
PGTI DS (6, 18, 27)	0+	171.28	164.64	181.05	0.36	0.44	0.34	0.02	0.01	0.01	4.23	3.99	3.98
Density	1+	459.78	460.18	462.48	0.84	0.84	0.86	0.01	< 0.01	0.01	6.95	6.79	6.71
	0+ 1+	649.65	647.82	657.62	0.84	0.84	0.83	< 0.01	< 0.01	0.01	6.03	5.84	6.01
PGTI DS (6, 18, 27)	0+	160.75	156.80	184.68	0.48	0.52	0.29	0.01	0.02	0.01	3.61	3.29	4.10
Discharge	1+	457.51	452.29	463.27	0.85	0.85	0.85	< 0.01	0.01	0.01	7.08	6.71	6.74
	0+ 1+	642.96	634.67	660.55	0.85	0.85	0.82	< 0.01	< 0.01	0.01	5.91	5.56	6.10
PGTI DS (6, 18, 27)	0+	164.61	156.90	185.50	0.46	0.53	0.32	< 0.01	0.01	0.01	3.88	3.51	4.01
Density	1+	454.48	447.02	466.27	0.85	0.86	0.85	0.01	0.01	0.02	6.88	6.49	6.79
Discharge	0+ 1+	638.85	626.27	662.00	0.85	0.86	0.83	< 0.01	< 0.01	0.01	5.87	5.49	6.08

Table 5. GLM – log model coefficients

	Coefficient (*β*)	Standard error	P-Value
Intercept	4.1439	0.0094	< 0.001
PGTI_Warming	0.2399	0.0080	< 0.001
Density	-0.0295	0.0105	0.005
Discharge	-0.0305	0.0082	< 0.001